



Iron deposits in the knee joints of a thalassemic patient

Citation

Economides, Charalambos P, Elpidoforos S Soteriades, Michalis Hadjigavriel, Ioannis Seimenis, and Apostolos Karantanas. 2013. "Iron deposits in the knee joints of a thalassemic patient." *Acta Radiologica Short Reports* 2 (1): 2047981613477401. doi:10.1177/2047981613477401. <http://dx.doi.org/10.1177/2047981613477401>.

Published Version

doi:10.1177/2047981613477401

Permanent link

<http://nrs.harvard.edu/urn-3:HUL.InstRepos:11855761>

Terms of Use

This article was downloaded from Harvard University's DASH repository, and is made available under the terms and conditions applicable to Other Posted Material, as set forth at <http://nrs.harvard.edu/urn-3:HUL.InstRepos:dash.current.terms-of-use#LAA>

Share Your Story

The Harvard community has made this article openly available.
Please share how this access benefits you. [Submit a story](#).

[Accessibility](#)

Iron deposits in the knee joints of a thalassemic patient

Charalambos P Economides^{1,2}, Elpidoforos S Soteriades^{1,3}, Michalis Hadjigavriel⁴, Ioannis Seimenis⁵ and Apostolos Karantanas⁶

¹Cyprus Institute of Biomedical Sciences (CIBS), Nicosia, Cyprus; ²Agios Therissos MRI Diagnostic Center, Department of MRI, Nicosia, Cyprus; ³Harvard School of Public Health, Department of Environmental Health, Environmental and Occupational Medicine and Epidemiology (EOME), Boston, MA, USA; ⁴Limassol General Hospital, Department of Internal Medicine, Limassol, Cyprus; ⁵Democritus University of Thrace, Medical School, Laboratory of Medical Physics, Alexandroupoli, Greece; ⁶University of Crete, Department of Medical Imaging, Heraklion-Crete, Crete

Correspondence to: Charalambos P Economides. Email: ceconomides@cibs.org.cy

Abstract

The overall prognosis for patients with β -thalassemia has improved considerably during the past decades mainly due to regular blood transfusions, improvements in chelation therapy, and enhanced surveillance with imaging studies examining iron overload and other clinical complications. However, the prolonged survival of these patients leads to the development of other health problems including degenerative diseases such as arthropathies, which require further attention since they have a significant impact on the quality of life. In the current case report, we present a 45-year-old white man with β -thalassemia complaining of non-traumatic pain and restriction in the range of motion of both knees. Magnetic resonance imaging (MRI) revealed a tear in the medial meniscus of the left knee as well as iron deposits in both knees. Histological findings confirmed the presence of hemosiderin in both joints. To our knowledge, this is the first reported case of macroscopically documented iron deposits in the knee joints of a patient with β -thalassemia using MRI.

Keywords: MR imaging, knee, arthritides, hematologic diseases

Submitted October 7, 2012; accepted for publication January 15, 2013

Patients with thalassemia constitute a significant public health problem. Providing comprehensive care to such patients has been viewed by many as a sensitive indicator of the level and quality of healthcare services in each country. Blood transfusions and iron overload of liver, spleen, and heart and their associated complications have received considerable attention by clinicians and researchers alike due to their significant impact on morbidity and mortality of these patients (1, 2). However, as the above problems have gradually been studied and appropriate therapies have been introduced in a relatively successful fashion, contributing to a dramatic increase of patients' overall survival, other health problems affecting quality of life eventually may require further attention. Such problems may be associated with aging and/or degenerative processes, which appear to have an accelerated pace in patients with β -thalassemia or may also be related to iron deposits in other organs including pancreas, pituitary gland, and joints (3, 4).

Arthropathy is one of the emerging chronic health problems affecting a significant number of patients with

β -thalassemia, which, so far, has received limited attention by the scientific, clinical, and public health community (2, 5–7). Although magnetic resonance imaging (MRI) has been regularly utilized in assessing iron deposits in liver, spleen, and heart and to a lesser extent in pancreas and pituitary gland, no studies have, to date, been published on the assessment of possible iron deposits in joints of patients with β -thalassemia (1, 3, 4, 8).

Case report

A 45-year-old white man with β -thalassemia major was referred for MRI of the left knee due to prominent non-traumatic chronic medial and lateral pain (past 1–2 years), as well as partial locking and restriction in the range of motion. Neither previous nor recent traumatic knee injury nor other suspicious events were reported. The patient had been undergoing regular blood transfusions twice a month maintaining a hemoglobin level of about 9.5 mg/dl and a ferritin level of 3000 ng/mL. The patient reported receiving chelation therapy with only oral deferiprone for

Table 1 Time trends of T2* measurements of liver and heart

Organ	Mean T2* (ms)			
	2007	2008	2010	2011
Liver [†]	3.8	4.2	1.6	1.6
Heart [‡]	18	22	11.3	10.3

[†]Iron deposits assessed by T2* liver measurements range from mild to moderate severity. Liver measurements were obtained from a region of interest prescribed in the segment V/VIII of the right liver lobe

[‡]Iron deposits assessed by T2* heart measurements range from normal to moderate severity. Heart measurements were obtained from a region of interest prescribed in the intraventricular region



Fig. 1 A fat-suppressed, PD-w image in the coronal plane of the left knee shows a longitudinal tear in the body of medial meniscus (long arrow) and the displaced meniscal fragment within the intercondylar notch (short arrow). In addition, osteoarthritic changes with minimal subcortical cyst formations and reactive bone marrow edema are noted in the medial tibial plateau (open arrow)

the past 13 years at a dose of 75 mg/kg/day. Occasional chelation with desferioxamine was also used during the same time period. T2* measurements from previous MRI examinations on heart and liver are presented in Table 1. It was evident from the decreasing T2* measurements of heart and liver, that there was progressive increase in the degree of iron deposits in the above two organs in parallel with clinical observations of poor adherence to chelation therapy compatible with high levels of plasma ferritin. Following regular assessment, the patient underwent MRI of the left knee. Subsequent MR scanning of the right knee was also performed for comparison purposes. Written informed consent was obtained from the patient for publication of this manuscript and accompanying images.

MRI technique

MRI was performed with a 3.0 Tesla scanner (Achieva, Philips Medical Systems, Best, The Netherlands) to assess

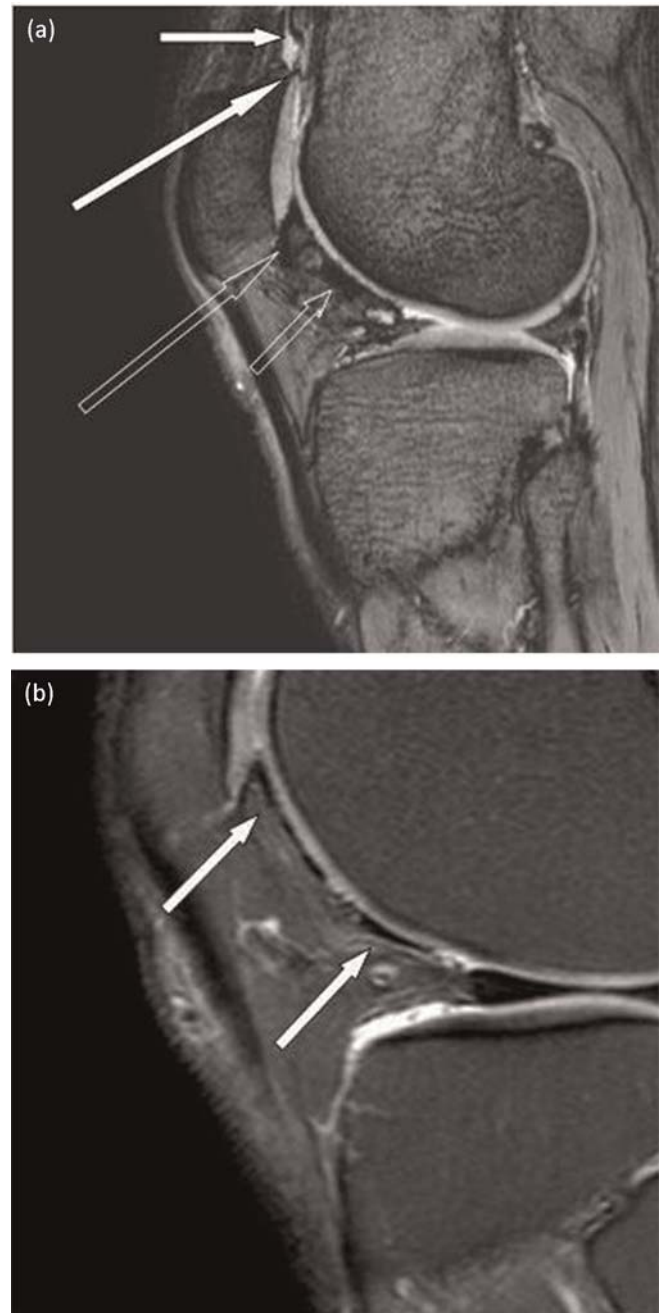


Fig. 2 (a) A T2*-w sagittal image in the left knee represents foci of iron deposits within the supra patellae pouch right above the superior pole of the patellae (short arrow) and also in contact with the patellae cartilage at the upper pole (long arrow), as well as within the Hoffa's fat pad in contact with the patellae cartilage in its inferior pole (open arrow) and in the cartilage surface over the trochlea (dotted arrow). (b) A fat-suppressed PD-w image in the sagittal plane in the left knee shows foci of iron deposition along the surface of the cartilage over the lateral trochlea (short arrow). We note the drop of signal in the area of iron deposits, which is less prominent in comparison with the corresponding T2*-w image

arthropathy including potential iron deposits in the knee joints. We used the built-in quadrature radiofrequency (RF) body coil and a phased array 8-channel knee coil for proton excitation and signal detection, respectively. MRI scanning protocol included several multislice pulse sequences routinely performed for morphological imaging

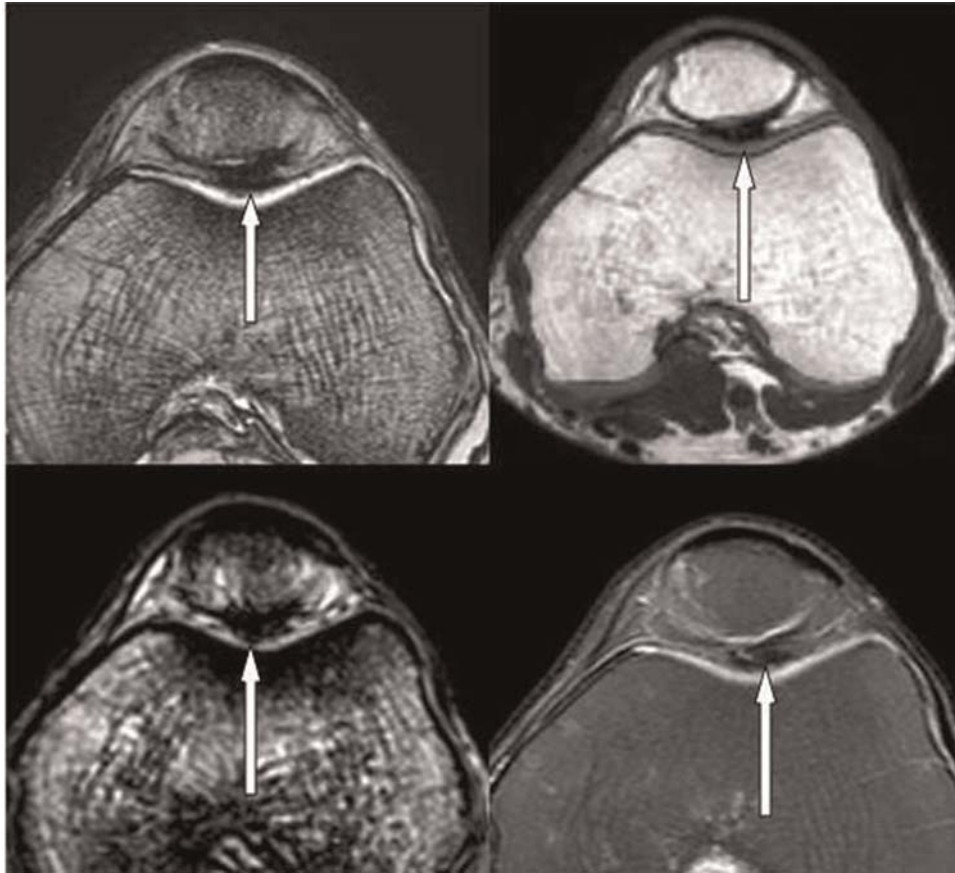


Fig. 3 This image represents four corresponding axial images from different pulse sequences of the left knee. (a) is a T2*-w image, (b) is an ultra short time echo (UTE) image, (c) was obtained with susceptibility weighted imaging (SWI), and (d) represents PD-w imaging with a turbo spin echo sequence. In (a), we note a large area of iron deposit in contact with the patellae and trochlea groove cartilage presented as a low signal intensity focus (arrow). In (b) and (c) we highlight a further exaggeration of the signal loss in the area of iron deposits on the UTE and SWI sequences, respectively (arrows). In (d) we note less conspicuous signal loss of the iron deposit area in the PD-w sequence (arrow)

(in each case, 28 slices were acquired with a field-of-view of 170 mm, a section thickness of 2.8 mm, and a pixel size of 0.6×0.7 mm); T1-weighted (T1-w) (repetition time [TR], 674 ms; echo time [TE], 18 ms; total scan time [ST], 2.5 min) turbo spin echo (TSE) in the sagittal plane; T2*-weighted (T2*-w) (TR, 575 ms; TE, 12 ms; ST, 2.4 min) gradient recalled echo (GRE) in the axial plane; proton density-weighted (PD-w) (TR, 2342 ms; TE, 35 ms; ST, 2.9 min) TSE with spectral fat suppression in the coronal and axial planes. Three-dimensional (3D) susceptibility weighted imaging (SWI) and ultra short echo time (UTE) GRE pulse sequences were also prescribed in the axial plane. The former utilizes an echo-shifting technique that allows the employment of relatively long echo times (TE, 21 ms) in a time-efficient way (TR, 15 ms; ST, 1.5 min for 100 slices with an acquisition resolution of $1 \times 1 \times 2$ mm). The latter uses a radial data sampling technique achieving an ultra short TE of $14 \mu\text{s}$ (TR, 7.5 ms; ST, 9.8 min; 144 slices; 1 mm^3 acquisition voxel size). The sequence used for quantitative T2 measurements was also prescribed in the sagittal plane. A single-slice (acquisition voxel size of $0.5 \times 0.5 \times 5.0$ mm) Carr Purcell Meibom Gill (CPMG) spin echo sequence employing 16 equidistant echoes, a short echo spacing of 6 ms and a TR of 2s was used (ST, 5.7 min).

MRI findings in the left knee

Left knee MR images revealed several pathological findings compatible with the prominent clinical symptomatology. The imaging findings included a flap tear of the medial meniscus with a displaced meniscal fragment in the medial intercondylar notch (Fig. 1). In addition, osteoarthritis was noted in the medial joint compartment with marked attenuation of the articular cartilage, reactive subcortical bone marrow edema in the medial tibial plateau, and minimal subcortical cystic changes (Fig. 1). Furthermore, there was mild attenuation of the patellar cartilage indicating chondromalacia patellae grade II. Foci of iron deposits were identified macroscopically within the supra-patellar pouch right above the superior pole of the patellae and also in contact with the patellae cartilage at the upper pole, as well as within the Hoffa's fat pad in contact with the patellae cartilage in its inferior pole and in the cartilage surface over the trochlea (Fig. 2a). Finally, iron deposits were also noted along the surface of the medial plica in the supra-patellar pouch. The iron deposits were detected as low signals intensity foci in all MRI sequences used. However, iron deposits were less conspicuous on the T1-w and PD-w sequences, with particular signal loss on gradient echo (Fig. 2B). During the above study we

Table 2 Measurements of T2 in different areas of the cartilage of the left knee

	Mean T2 (SD) (ms)			
	Patella	Lateral trochlea	Articular surface (lateral femoral condyle)	Articular surface (lateral tibial plateau)
Time (ms)	60 (11.5)	79 (8.8)	63 (18.6)	40 (8.9)

also noticed further exaggeration of the signal loss on the SWI and UTE sequences (Fig. 3). In Table 2 we present mean T2 measurements for regions of interest prescribed in different areas of the cartilage in the left knee. The T2 measurement of normal Hoffa's fat pad was 215 ms (18.8 SD), while in Hoffa's fat pad with iron deposits T2 measurement was 54.8 ms (11 SD) and in the supra-patellar pouch with iron deposits T2 was 51.1 ms (4.4 SD), respectively. Such findings indicate iron deposits in the above regions with decreased T2 measurements.

MRI of the right knee was also performed mainly for comparison purposes. Iron deposits were also noted in the right knee (Fig. 4). Iron deposits were noted in contact with the inferior pole of the patellar cartilage, as well as in contact with the anterior articular surface of the lateral femoral condyle.

Histology results

Following MRI studies, the patient underwent an arthroscopy of the left knee in order to explore the pathological imaging findings and repair the meniscal tear. Biopsy of the synovium showed edema of the basal membrane with papillary morphology and hemosiderin deposits. Histiocytes with hemosiderin moieties were also noted along with hyperplastic serous cells.

Discussion

To our knowledge, this is the first reported case of iron deposits in the knee joint of a patient with β -thalassemia major potentially associated with clinical symptoms. Our case report poses an important question regarding the prevalence of iron deposits in knee and other major joints of patients with β -thalassemia major, especially those of the lower extremities. In addition, this particular case raises further clinical concerns as to whether iron deposits in joints may be associated with clinical arthropathy in such patients. Furthermore, we pose a scientific question on the potential association of iron deposits in joints leading to the development of synovitis and/or cartilage damage (2, 5–7). Finally, our findings lead to significant clinical questions with respect to the effectiveness of the traditional chelation therapy to remove iron deposits from the joints of patients with β -thalassemia.

The examination of our case was facilitated by MRI techniques based on the GRE method that allow the visualization of small foci of iron deposits. Such techniques include



Fig. 4 A T2*-w sagittal image of the right knee obtained with a gradient recalled echo (GRE) pulse sequence. Iron deposits are noted in contact with the inferior pole of the patellae cartilage (short arrow), as well as in contact with the anterior cartilage surface of the lateral femoral condyle (long arrow)

the traditional T2*-w as well as the novel UTE and SWI methods (9). The high sensitivity of the UTE pulse sequence to iron is due to the ultra short echo time that employs, which allows visualization of short T2 species. SWI is also a relatively new MRI sequence, which evaluates and exploits the magnetic properties of tissues. Paramagnetic substances like deoxyhemoglobin, a product of blood degradation, and ferritin, a non-heme iron, are known sources of magnetic susceptibility in the tissues and they appear as hypointense foci. Albeit the high sensitivity of UTE and SWI sequences in the detection of iron deposits, CPMG and GRE sequences are more suited for quantitative imaging in tissues, since the presence of paramagnetic species reduce regional transverse relaxation times. Therefore, T2 and T2* measurements are widely used for liver and heart iron load evaluation.

As UTE and SWI are much more sensitive at lower concentrations of iron, they can be used to detect small foci of iron deposits that conventional spin echo and GRE pulse sequences fail to depict. In addition, because of their 3D nature, UTE and SWI offer the possibility of rigorous and thorough inspection of the joint for iron. Thus, they can effectively guide the correct prescription of the single-slice sequences used for quantitative transverse relaxation time measurements. Due to the negative contrast effect of iron foci, a major challenge is to distinguish regions of signal void due to iron from those due to low signal tissues or susceptibility artifacts. Therefore, T2 measurements were only performed at regions which appeared hypointense in both UTE and SWI images.

MRI and the documented pathological picture of the left knee, excluding the meniscal flap tear, showed advanced

degenerative changes, which are thought to be non-compatible with the patient's age and clinical history. This is an interesting finding in view of the macroscopically noted iron deposits and the poor adherence to chelation therapy. Further studies are warranted in order to examine the prevalence of iron deposits in the joints of patients with β -thalassaemia and their potential association with accelerated degenerative changes especially in the lower extremities. In addition, there should be enhanced clinical interest on the evaluation of the effectiveness of chelation therapy for removing iron deposits from joints in a similar fashion with other organs such as liver and heart.

Our case report, although raising important epidemiological and clinical questions, may not be representative of the majority of patients with β -thalassaemia in the developed countries, where patients may adhere to chelation therapy, since the particular patient had a poor adherence to chelation treatment. An additional limitation of our case may be associated with our inability to dissociate the documented clinical pathology in the knee joint with the degenerative changes and allocate potential partial etiology to iron deposits. Although the case is an interesting example of iron deposits in knee joints, the causal relationship with arthropathy/meniscal rupture documented with MRI and arthroscopy is purely speculative. Further epidemiological studies with case series, case-control, and cohort studies are warranted to explore the above scientific questions.

In conclusion, our case report highlights a new and emerging chronic problem of patients with β -thalassaemia; namely arthropathy, which may be potentially related to accelerated degenerative changes in the joints of the above patients in association with iron deposits.

ACKNOWLEDGEMENTS

The authors thank Philips Medical Systems Inc., Best, The Netherlands for their kind provision of the ultra short TE pulse sequence.

REFERENCES

- 1 Anderson LJ, Westwood MA, Prescott E, *et al.* Development of thalassaemic iron overload cardiomyopathy despite low liver iron levels and meticulous compliance to desferrioxamine. *Acta Haematol* 2006;**115**:106–8
- 2 Chan Y, Li C, Chu WC, *et al.* Deferoxamine induced bone dysplasia in the distal femur and patella of pediatric patients and young adults: MR Imaging Appearance. *Am J Roentgenol* 2000;**175**:1561–6
- 3 Anderson LJ, Westwood MA, Holden S, *et al.* Myocardial iron clearance during reversal of siderotic cardiomyopathy with intravenous desferrioxamine: a prospective study using T2* cardiovascular magnetic resonance. *Br J Haematol* 2004;**127**:348–55
- 4 de Assis RA, Ribeiro AA, Kay FU, *et al.* Pancreatic iron stores assessed by magnetic resonance imaging (MRI) in beta thalassaemic patients. *Eur J Radiol* 2012;**81**:1465–70
- 5 Chand G, Chowdhury V, Manchanda A, *et al.* Deferiprone-induced arthropathy in thalassaemia: MRI findings in a case. *Indian J Radiol Imaging* 2009;**19**:155–7
- 6 Berkovitch M, Laxer RM, Inman R, *et al.* Arthropathy in thalassaemia patients receiving deferiprone. *Lancet* 1994;**343**:1471–2
- 7 Kellenberger JC, Schmugge M, Saurenmann T. Radiographic and MRI features of deferiprone related arthropathy of the knees in patients with β -thalassaemia. *Am J Roentgenol* 2004;**182**:989–94
- 8 Noetzli LJ, Panigrahy A, Mittelman SD, *et al.* Pituitary iron and volume predict hypogonadism in transfusional iron overload. *Am J Hematol* 2011 Nov 4 [Epub ahead of print]
- 9 Hall-Craggs MA, Porter J, Gatehouse PD, *et al.* Ultrashort echo time (UTE) MRI of the spine in thalassaemia. *Br J Radiol* 2004;**77**:104–10